Conference Paper, Published Version

Baez Rivero, Ines; Jarquin Laguna, Antonio; Bricker, Jeremy

Robustness of J-type vs. U-type Oscillating Water Column Breakwaters

Coastal Structures 2019 - Nils Goseberg, Torsten Schlurmann (eds) - © 2019 Bundesanstalt für Wasserbau
ISBN 978-3-939230-64-9 (Online) - DOI: 10.18451/978-3-939230-64-9_004

Robustness of J-type vs. U-type Oscillating Water Column Breakwaters

I. Báez Rivero, A. Jarquin Laguna & J. D. Bricker
Dept. of Hydraulic Engineering, Faculty of Civil Engineering & Geosciences, Delft University of Technology, Delft, the Netherlands

Abstract: Typically, oscillating water column (OWC) breakwater design is focused on optimization of efficiency in the design wave regime. However, damage to OWC's during storms has been a major roadblock to further implementation of OWC technology. Here we compare J-OWC and U-OWC designs, and their behavior under extreme wave conditions. The first phase of this work is validation of the ANSYS Fluent computational fluid dynamics (CFD) model against laboratory experiments of an OWC near resonance at design operating conditions. In the second phase of this work, CFD is applied to investigate the response of the OWC to the extreme wave conditions experienced by the Mutriku OWC in Spain during the storm of 2009. Finally, stresses and displacements in the caisson walls are analyzed using MIDAS Civil structural analysis software. We find that the U-OWC is much better protected from storm waves than the J-OWC, while the resonant response of the U-OWC is slightly attenuated.

Keywords: Wave Energy Converter (WEC), Oscillating Water Column (OWC), Structure robustness, Caisson Breakwater, ANSYS Fluent

1 Oscillating Water Column

Wave power is a pollution-free way to generate electricity. The usage of Oscillating Water Columns (OWC) in Coastal Structures such as caisson breakwaters, is an efficient and sustainable way to generate wave power, combined with coastal protection of the shoreline, having little impact on aquatic life and easy maintenance access (Falcao, 2010).

The OWC is recognized internationally as one of the most promising types of wave energy converter (WEC) (Elhanafi & Joo Kim, 2018). The OWC is a partially submerged structure device, with a bottom opening to allow wave energy to enter and then transform that energy into electricity. The opening at the bottom of the column is located slightly below the minimal water level, allowing waves to enter. The water level inside the column fluctuates with the incident wave, and thanks to the resonance produced in the OWC, the water level fluctuation inside the OWC is enhanced. At the top of the OWC there is an air chamber, which compresses air as the water level rises and decompresses the air as the water level drops. The difference in air pressure drives an air turbine, which is responsible for the mechanical energy conversion into electricity (Mustapa, et al., 2017).

1.1 Operation near resonance conditions

The efficiency of an OWC is highly related to its resonance with the incoming wave state. The resonant frequency of an OWC will determine the wave state at which device generates energy most efficiently. This depends on the wave excitation and the geometry of the OWC, which determine the amplitude of the oscillation inside the water column. For frequencies well above the resonant frequency, the column of water in the OWC will not have time to react to the oscillation, generating almost no motion in the caisson. Also, for frequencies below the resonance, the body of water will behave as quasi-steady, following the vertical motion of the incoming waves, without resonance. Only within a specific range of wave frequencies does the oscillation in the OWC give high levels of

resonance and thus the most efficient wave energy conversion. This range of frequencies is related to the submerged depth, and, the geometry of the OWC (Kamath, et al., 2015).

1.2 Air turbines

In general, the air turbines used for OWC-breakwaters are Wells or impulse turbines or variations of these (Webb, et al., 2005). The main advantage of the commonly used Wells turbine is its bidirectional allowance, which means that regardless of the direction of air flow through the turbine, this will still rotate in the same direction. The impulse turbine is a self-pitched controlled turbine with guide vanes. Guide vanes are pivoted and can rotate freely. When airflow changes direction, these guide vanes change their orientation to meet the right position according to the airflow, acting as a nozzle or diffuser for each situation. This type of turbine has a more complex design and operation than the Wells turbine, and so if the guide vanes fail in their function the whole system fails (Czech & Bauer, 2012).

1.3 Designs: J-type and U-type

The integration of OWC's in sea defense structures is a cost-effective measure. In particular, the caisson breakwater is the most popular option, due to its simplicity and durability. For caisson breakwaters, the orientation is usually perpendicular to the incoming wave direction, causing partial reflection when waves break on the flat surface. By integrating an OWC, wave energy normally dissipated or reflected by the breakwater, can be transformed into electricity (Mustapa, et al., 2017).

There are two examples of breakwater-integrated OWC constructions that have achieved expected results. The first construction of an integrated OWC structure is the Sakata breakwater, built in Japan in 1990. The design used is called a J-OWC. Another example of this design is the OWC caisson breakwater completed at the port of Mutriku in Spain in 2009.

The design of an OWC is complex, and presents various uncertainties. Despite years of implementation and development of new designs, several trouble spots persist. A general design is not feasible, as design depends on site-specific characteristics. In general; projects are small, so do not reach a cost effective status (Arena, et al., 2013).

The newest OWC design is the U-OWC, developed from the J-OWC with an additional wall. Arena, et al., (2013) suggest the U-OWC can show better performance than the J-OWC. Figure 1 and Figure 3 show J- and U-OWC designs.

1.4 Robustness and Failure Mechanisms

Some OWC breakwaters have collapsed under extreme wave conditions. This is the case of the construction at Mutriku in the Basque Country in Spain. This J-OWC construction started in 2005 and suffered five storms between 2007 and 2009 (Berenguer, 2009). For the storm in 2009, the structure did not resist as expected and severe damage lead to failure of four of its sixteen OWC chambers. Cracking in the concrete structure, especially in the joints connecting different components, lead to failure of the entire front wall for four of the chambers (Torre-Encino, et al., 2010).

2 Methods

The purpose of this paper is to analyze the performance of different OWC designs under extreme wave conditions, studying the efficiency and structural response/robustness of OWC under wave loads of different magnitude for structural optimization. In order to do so, physical and numerical modelling are required. The laboratory experiments validate a numerical model at design wave conditions. The numerical model then allows us to reproduce extreme wave conditions and compare the behavior of different designs. This analysis will facilitate improved design and robustness of the structure under extreme wave loads.

To compare the structural designs of J-type and U-type OWC designs, the conditions experienced at Mutriku (Spain) during the storm of 2009 are considered, and to investigate wave pressures exerted on the OWC structure and determine the best structural option for robustness under extreme wave conditions.

2.1 Experimental Set-up of the Laboratory Tests

Since the Mutriku design is well documented, it is taken as a reference for the physical experiments. The Froude scale is used for the laboratory experiments, carried out at a scale of 1:25. The dimensions of the wave tank at TUDelft Water Laboratory are 39 meters of effective length, 0.8 meters width and 0.85 m depth. The wave generator at the wave tank is a hydraulic driven piston, which allows automatic reflection compensation. The wave conditions considered for the laboratory experiments are presented in Table 1.

Tab. 1. Wave conditions of laboratory experiments

Case	Water level (m)	H_s (m)	T_p (s)
1	0.47	0.05	1.7
2	0.47	0.05	1.8
3	0.47	0.05	1.9
4	0.47	0.05	2.0
5	0.47	0.05	2.1
6	0.47	0.05	2.2
7	0.47	0.05	2.3
8	0.47	0.05	2.4
9	0.47	0.05	2.5

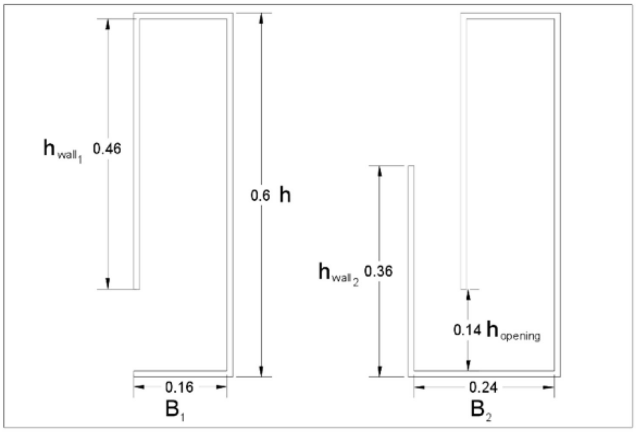

Fig. 1. Detail of laboratory model dimensions – J-type (left), U-type (right).

Pressure sensors are located in three different walls of the OWC. One in the front wall, to register the pressure of the incoming wave. A second pressure sensor is located in the back wall, to allow a better understanding of the incoming wave energy reaching the inside of the air chamber. The third pressure sensor is located at the top wall of the model, which will give information on the air compression occurring in the chamber. Also, a set of wave gauges are located at different points along the wave tank, to check the incoming wave at three, seven and eleven meters in front of the model. Figure 2 shows the location of the pressure sensors in the physical model.

Fig. 2. OWC model in the Laboratory facilities at TUDelft (left – front view - showing the front pressure sensor, right – back view – showing the back and top pressure sensor).

Three different configurations of the OWC laboratory model top cover are used for both the J-type and U-type OWC, giving a total of six different scenarios to be tested in the laboratory experiments.

- The first scenario is the J-type OWC with the top cover fully closed, see Figure 3 top image. The top cover pressure sensor facilitates understanding of the relation between the incoming wave and the air compression in the air chamber.
- Another set of experiments is carried out but without the top cover of the OWC, the top of the model is fully open in this case. This allows us to incorporate a wave gauge inside the OWC

and analyze the resonance in the OWC relating the incoming wave with the water level inside the OWC.

- A third set of experiments presents a transverse opening in the top cover. An OWC incorporates a turbine, normally a wells turbine, which is connected to the air chamber. The presence of a turbine partially restricts the flow rate of the outgoing air. In order to represent this restriction, and based on the Mutriku design and dimensions, an opening in the top cover represents the turbine. Through the top opening a wave gauge measures the water level in the OWC, which compared to the results of the experiment with the open top, will give a better idea of the effect of the turbine with the resonance, which is directly related to the efficiency of the OWC.

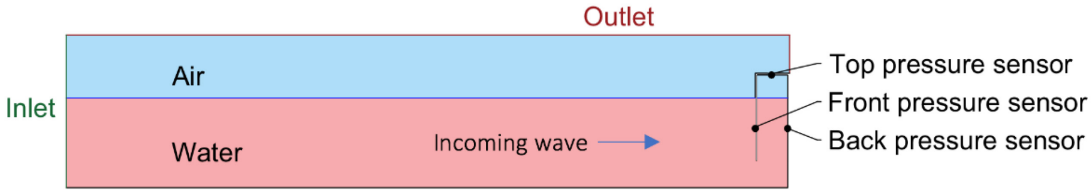

Fig. 3. Cross section of the geometries Geometries of the J-OWC (top) and U-OWC (bottom) and location of the pressure sensors in the different walls.

These three sets of experiments with different top covers are executed for the two different OWC structure designs, J-OWC and U-OWC, giving a total of six different scenarios. Figure 3 shows the J-type and U-type OWC designs for the top cover fully closed.

2.2 CFD - Computational Fluid Dynamics with ANSYS Fluent

Wave generation is simulated using ANSYS Fluent model version 18.2 (ANSYS, 2009). The numerical model is validated against the laboratory experiments for design waves, and then used to investigate extreme wave conditions that could not be simulated in the laboratory. Validation to design conditions also provides information on the limitations of ANSYS Fluent.

2.2.1 Set-up of the Numerical Model of the OWC with ANSYS Fluent for Validation

Figure 4 presents a section of the ANSYS Fluent wave tank for the J-OWC fully open scenario (the full domain stretches further to the left, to replicate the full length of the laboratory wave flume, but is trimmed here for clarity of the OWC section). The model is divided in three areas with different mesh sizes; where in Area 1 mesh face size is 0.15 m, Area 2 right center and bottom is 0.0025 m and Area 3 left center is 0.005 m.

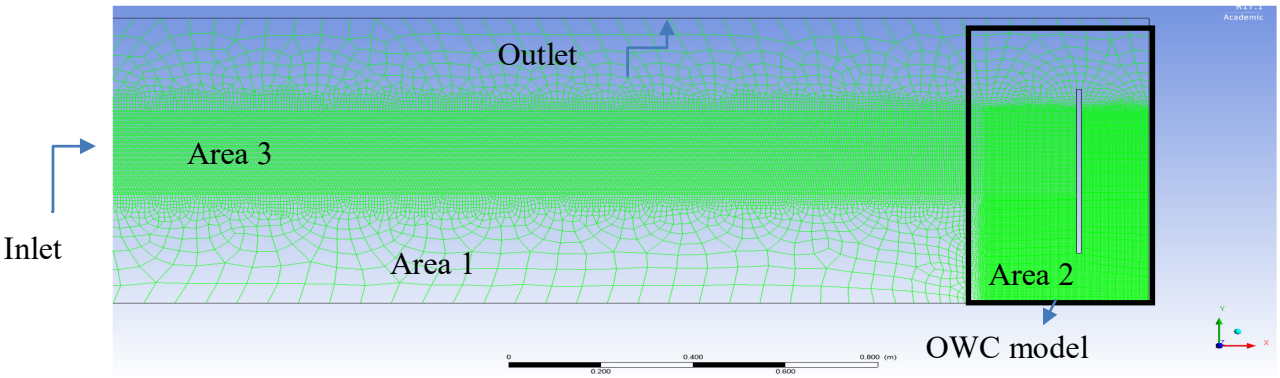

Fig. 4. Section of the ANSYS Fluent mesh (see Table 3 for detailed information).

The inlet is an open channel wave boundary condition, with regular second order stokes waves. The primary phase at the top of the flume is air, and the bottom where the fluid propagates is defined as the secondary phase (water). The Inlet is on the left, where waves are defined with a “velocity inlet” boundary condition. The top of the flume and a small area of the top of the right wall, above the OWC, are defined as “pressure outlet” (atmosphere). Other important factors to consider are that the

model is two dimensional (transverse averaged), and a k-epsilon turbulence model is used for these tests. In addition, a compensatory outflow is required to compensate for the Stokes Drift at the open boundary. Otherwise the wave flume in ANSYS will gradually fill up with water.

A summary of the boundary conditions is provided in Table 2, and the characteristics of the geometry and mesh are provided in Table 3.

Tab. 2. Boundary conditions summary

General		**Fluids**	
Type	Pressure-based	Air	Primary phase
Velocity formulation	Absolute	Water	Secondary phase
Time	Transient	**Boundary Conditions**	
2D Space	Planar	Inlet	Type: Velocity - inlet
Gravity	Y: -9,81 (m/s^2)	Outlet	Type: Pressure – outlet
Multiphase	Open Channel Wave BC	Wave conditions	Short Gravity Waves
Viscous model	k-epsilon model	Wave theory	Second Order Stokes
Compute from	Inlet	Initiation method	Standard Initialization
Open channel initialization method	Flat	Compute from	Inlet
		Open channel initiation	Flat

Tab. 3. Characteristics of the geometry and mesh sizing for ANSYS Fluent for Mutriku case (related to Figure 4)

Characteristics of the model	**Bounding box**	**Characteristics of the mesh size**	Bounding box
Length x	87.75 m	Max Face size (Area 3)	2.0 m
Length y	93.7 m	Area 1 (Center)	0.0015 m
Length z	0 m	Area 2 (top and bottom around area 1)	0.7 m
Surface Area	7103 m^2		
Nodes	313014		
Elements	312202		

3 Results

Validation of the results obtained with fluent ANSYS Fluent is necessary to confirm that the performance and outcomes match with the physical model, confirming also that the boundary conditions defined in ANSYS Fluent match with reality. Pressure sensors are located in the front and back walls of the OWC laboratory model, so these can be compared with the ANSYS-Fluent results. The water level inside the OWC is also compared, to validate the resonance behavior for different wave scenarios.

3.1 J-OWC Shape Validation – Fully Open

For validation of the J-OWC, laboratory experiments covered periods from 1.7 sec to 2.5 sec for a wave height of 0.05 m. Figure 5 shows results for the front wall pressure sensor (see Figure 2 for location of front wall pressure sensor). In general, the results coincide well, Table 4 shows the results corresponding to Figure 5.

Figure 6 shows the validation for the back-wall pressure sensor (see Figure 2 for location of the sensor). Notice that the back-wall pressures present higher values. Therefore, inside of the J-OWC, pressures are generally higher than outside near design conditions. This confirms, as stated by Müller and Whittaker (1995), the wave pressures acting on the back

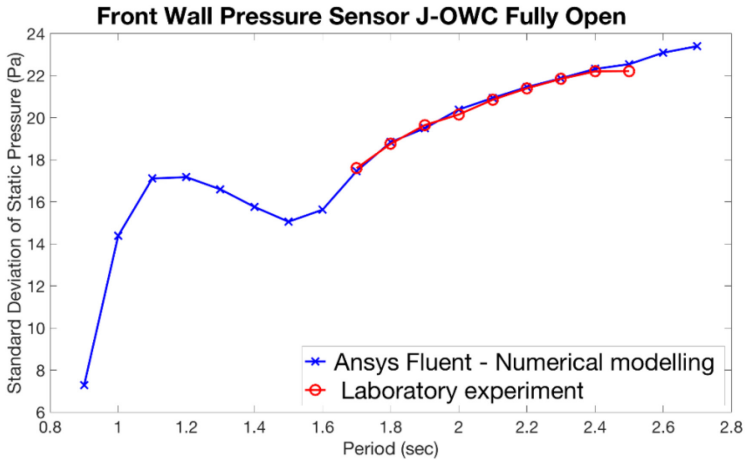

Fig. 5. Validation of ANSYS-Fluent results for the front wall pressure sensor for a J-OWC when the top cover of the OWC is open.

wall are higher than those acting on the front wall, due to the flow field and the reflectivity (Boake, et al., 2002). Resonance inside the J-OWC for an incident wave height of 0.05 m, is maximum at a period of 1.7 sec (Figure 7).

Tab. 4. Numerical results for the front wall pressure sensor for a J-OWC when the top cover is fully open (related to Figure 5)

	Standard Deviation of Static Pressure (Pa)	
Period (sec)	**ANSYS Fluent**	**Laboratory experiments**
0.9	7.3	-
1	14.2	-
1.1	1.7	-
1.2	1.7	-
1.3	16.6	-
1.4	15.8	-
1.5	15	-
1.6	15.7	-
1.7	17.7	17.8
1.8	18.7	18.7
1.9	19.7	19.68
2	20.05	20
2.1	20.3	20.3
2.2	21.6	21.6
2.3	21.9	21.9
2.4	22.05	22
2.5	22.1	22
2.6	23.1	-
2.7	23.4	-

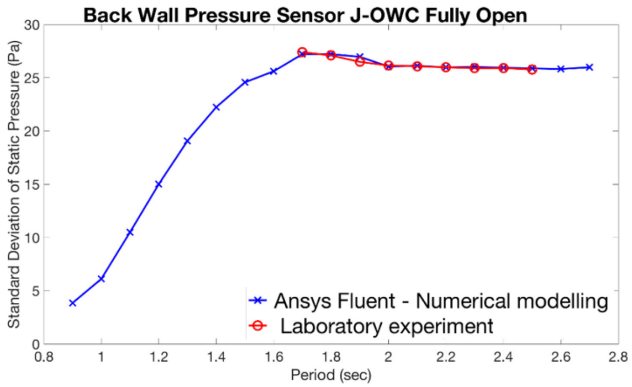

Fig. 6. Validation of ANSYS-Fluent results for the back-wall pressure sensor for a J-OWC when the top cover of the OWC is open.

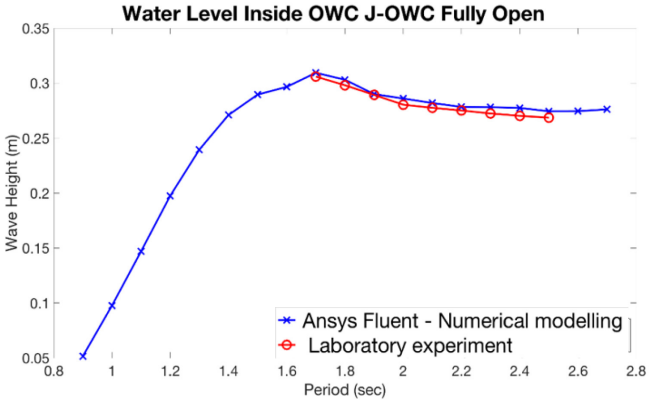

Fig. 7. Validation of ANSYS-Fluent results for water level inside of a J-OWC when the top cover of the OWC is open.

3.2 J-OWC Shape Validation – Partially and Fully Closed

In the case of a J-OWC when the top cover is partially open, the level of resonance inside reduces in comparison to the fully open setup. The partially open scenario is a more realistic representation, approximating resistance from a turbine. ANSYS Fluent assumes the air to be incompressible, therefore, the validation of the fully closed case is not considered. This fact also affects the partially closed scenario, which might help explain the higher wave heights in the CFD than in the laboratory.

3.3 U-OWC Shape Validation – Fully Open

This sub-section presents the results obtained from a comparison of the results for the physical and numerical model with a U-OWC design. The front pressure sensor on the U-OWC in Figure 8 - a, shows similar trends for the laboratory and the ANSYS Fluent results. Figure 8 - b, showing the

comparison of the back-wall pressure sensor, shows good agreement at shorter periods. However, at longer wave periods, it shows a disagreement in the values. As the period increases, ANSYS-Fluent back wall pressure increases more than in the laboratory experiment.

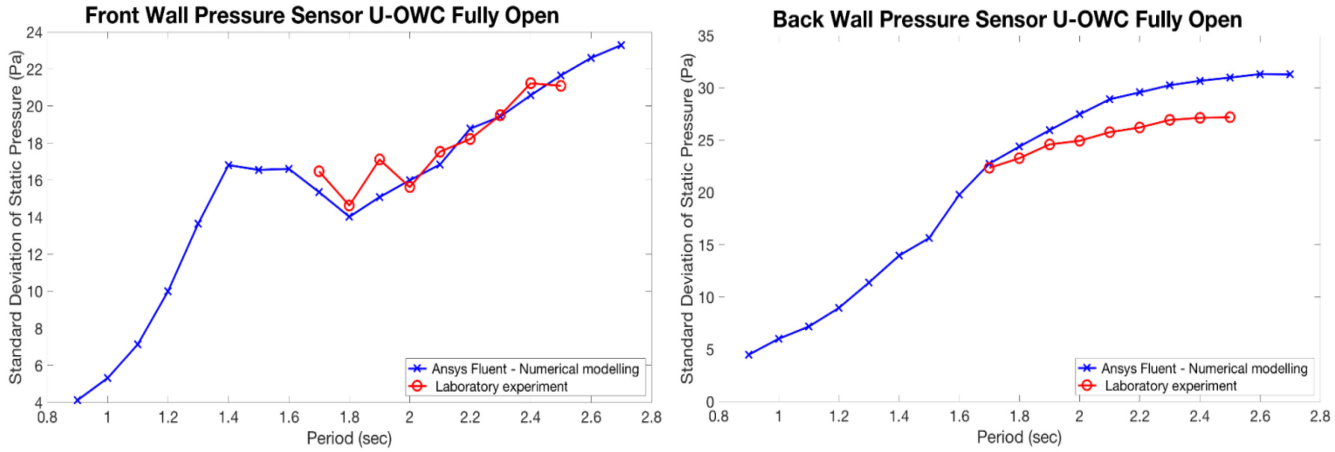

Fig. 8. Validation of ANSYS-Fluent results for a U-OWC when the top cover of the OWC is open, the front wall pressure sensor (Figure 8 – a, left) and for the back wall pressure sensor (Figure 8 – b, right).

3.4 Results: Structural –Extreme Waves at Mutriku OWC

The ANSYS-Fluent numerical model is then run for the different OWC geometries under extreme wave conditions based on the Mutriku storm conditions provided by the Basque Government (Torre-Encino, et al., 2010). Four combinations of waves are compared; High and Low mean water levels with regular waves of 8 and 13.7 meters height (HWL and LWL are shown in Figure 9).

For each wave condition, static pressures values in the structure are applied in MIDAS Civil software (Torkar & Jeszenszky, 2006), for structural analysis of the front and back walls. MIDAS is a finite element software that solves beam elements for displacement and maximum stress at intermediate points or end nodes.

In order to obtain a more accurate comparison of the pressures in the structure for the different scenarios, instantaneous static pressures with ANSYS Fluent are extracted at 16 different points along the structure at the moment of average maximum peak pressure (Figure 9 – f shows the 16 pressure points selected in burgundy circles).

At Low Water Level with waves of 13.7 meters height shown in Figure 9, a strong decrease in internal pressures with the presence of a U-wall design is noticeable. The simplest design of a J-OWC (Figure 9 – a), for which the pressures inside the OWC are high, may lead to failure of the structure due to the high pressure inside pushing out the walls of the OWC. With the presence of a front U-wall of four meters height (Figure 9 – b), which is the lowest U-wall considered, the internal pressures in the OWC reduce drastically. High pressure is exerted on the outside of the front wall of the OWC at the same level as the crest of the U-wall. Figures 9 b, c, d and e show examples with 1 meter increments in the U-wall height up to seven meters. It is noticeable that high pressures on the outside of the front wall are highest at the crest of the U-wall. Also noticeable is that internal OWC pressures are low compared to the J-OWC, for all U-wall heights.

With the static results from ANSYS Fluent, structural analysis of the front and back walls is performed with MIDAS Civil. Beam stresses and displacement resulting from the CFD-modeled pressures are calculated. The failure of the Mutriku OWC structure was due partially to the failure of joints between precast concrete parts and the in-situ construction, and due partially to possible fracture of the concrete by shear stresses, causing cracking at specific locations. The true shear strength of concrete is difficult to determine because it is normally affected by other stresses in the structure. Therefore, displacements of the walls are presented, which, with further information on the stresses in the joints could be used to investigate the failure limit for the front and back walls.

From the MIDAS Civil results, the analysis shows that the J-OWC design is the most vulnerable, with the front wall suffering the most displacement (0.016 m). In the case of the U-OWC design, the displacement is reduced, see results in Table 5.

MIDAS Civil analysis shows a considerable reduction in front wall displacement for all of the U-OWC geometries compared to the original J-OWC. The U-OWC with a 4 m U-wall experiences the lowest front wall displacements of all the geometries investigated. For the back wall, again the maximum displacement is experienced by the J-design, with a considerable displacement reduction for the U-OWC designs. The displacement reduction is up to 90% for the 4 meter U-wall at low water level (LWL) with 8 meter wave height.

Tab. 5. MIDAS Civil displacement results of the front wall

Type of OWC	Front wall	Displacement (meters)
J	0 meters	0.016
U	4 meters	0.0019
	5 meters	0.0036
	6 meters	0.002
	7 meters	0.0024

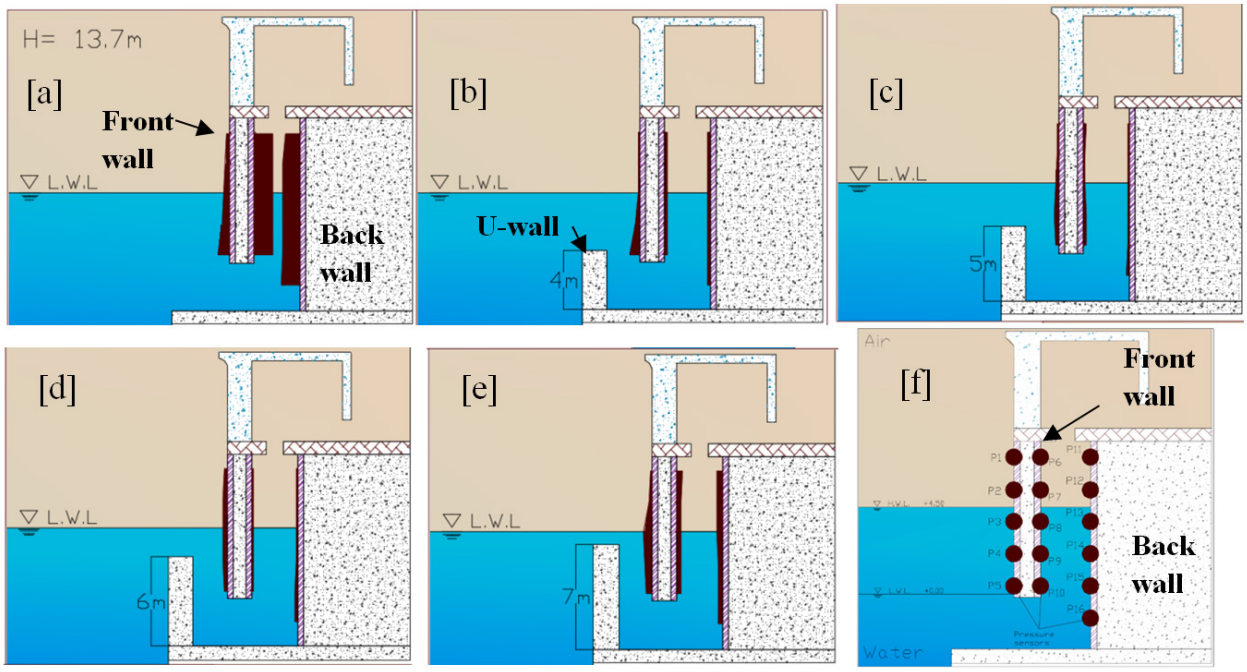

Fig. 9. a b c d and e: Comparison of the five different geometries for 13.7 meters wave height at High Water Level. 2 – f shows the pressure data extraction points.

4 Discussion: Limitations and Recommendations

Major limitations of this research are:

- The laboratory experiments carried out were limited in the range of wave conditions to avoid splashing of the water over the wave tank side walls, leading to limitations in the wave periods that were used. Higher panels on the side of the wave tank could be a simple solution to this.
- The academic version of ANSYS Fluent restricts the number of cells to 500,000, effectively limiting the numerical analysis to two dimensions.
- The Midas Civil structural analysis was performed for a one-dimensional structure. Consequently, the front wall, which is in reality attached to the OWC at its top and side edges, is in the structural analysis considered as a cantilever concrete beam, only attached at the top. A similar limitation happens with the back wall, which is in reality attached to the rest of the structure on all four edges, but Midas civil analysis is carried out in 1D, and therefore, only the top and bottom attachment points are considered.

Recommendations for further research are:

- To improve the U-OWC validation, further analysis of the numerical modelling comparing different wall frictions should be implemented. Figure 10 shows the original full-slip results, compared to numerical models accounting for wall friction. The model result with wall friction is closer to the laboratory experiment, but still not as accurate as the J-OWC result.

- The incorporation of a partially open top cover of an OWC, aims to represent the OWC behavior with a turbine integrated in the system. The opening chosen for the cover is arbitrary, and not an accurate calculation of the dimensions required to accurately represent the behavior of a wells turbine or any other turbine type. This analysis can certainly be improved, and more realistic resistance simulated.
- Numerical analysis of more extreme wave conditions and water levels. A wider variety of wave conditions, with different wave heights and different water levels for each geometry, could give a better understanding on the behavior of the water with the front vertical duct and a better final analysis to determine the best design alternative.
- Analysis of wave pressures for a U-OWC with a lower front wall. The U-OWC with a 4 m high wall showed the best results in extreme wave conditions. Therefore, it would be helpful to consider even lower walls.
- The structural analysis carried out with Midas Civil is a simple static 1D analysis, which could be improved to a dynamic 2D analysis.
- The pressure information from the front and back walls is applied in Midas Civil as point loads and not as distributed loads. This should be considered, and further analysis of the structure with distributed pressures can be implemented.

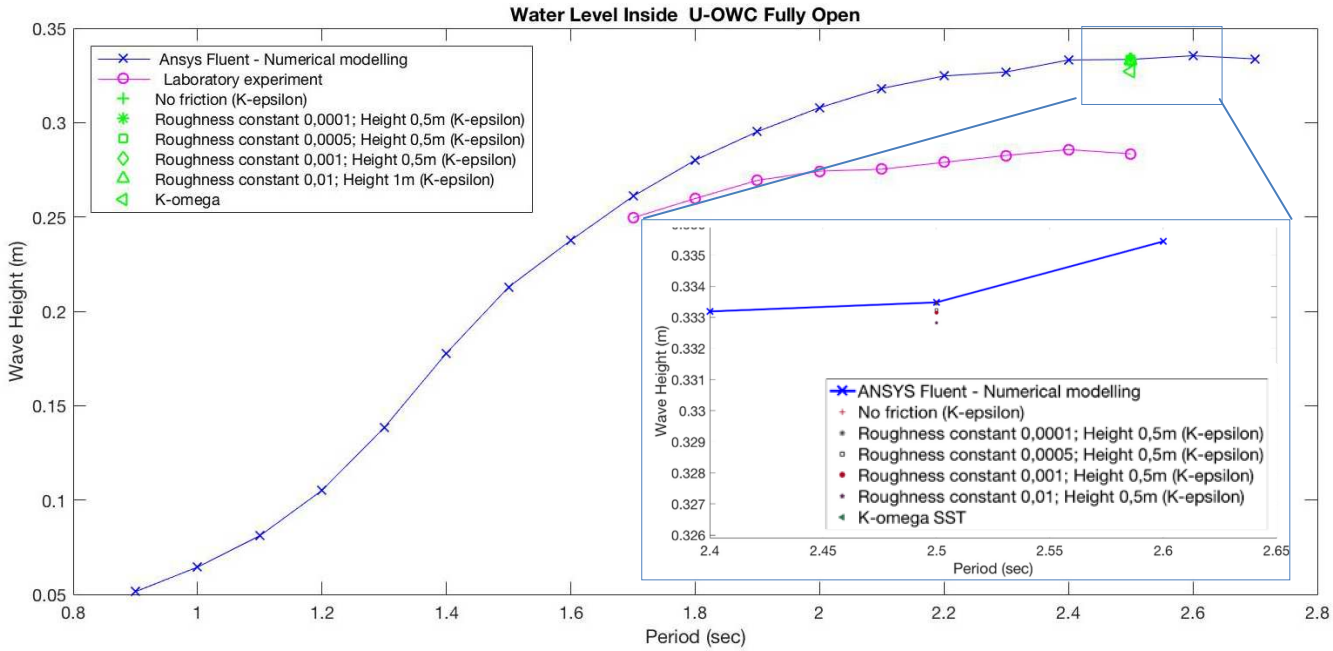

Fig. 10. Comparison of the validation of ANSYS-Fluent results for wave height inside of a U-OWC with an open top, with different wall friction values.

5 Conclusions

How well does the numerical simulation represent the physical experiments at design wave conditions?

The validation of the J-OWC is very accurate, but the validation of the U-OWC is not as precise, even though all experiments and simulations were identical other than for the OWC geometry. This could be due to the friction of the OWC walls. As the J-OWC has the fewest walls, the interaction of the fluid with the OWC walls is a minimum for the J-OWC. On the other hand, the U-OWC includes a narrow vertical duct in front of the OWC, making wall friction have more of an effect on the U-OWC than on the J-OWC. This wall friction was not considered in the initial numerical ANSYS-Fluent model (wall surfaces were modeled as full-slip), which can explain why the results for the J-OWC are more accurate than for the U-OWC.

5.1 Comparison of a partially closed top cover versus an open top cover on the J-OWC

The model OWC with a partially closed top cover more realistically simulates an actual OWC than the model with a fully open top, because an actual OWC has a turbine that provides resistance to the air flow into and out of the OWC air chamber. Our results show that the partially closed top cover reduces the amplification inside the OWC, compared to a fully open top. This reduction is especially evident at the resonant peak period of 1.7 sec.

5.2 Comparison of geometries

The results of this study show that the pressures affecting the internal structure of the OWC are reduced when using a U-OWC as compared to a J-OWC. The U-OWC experiences lower total displacement and beam stresses of the front and back walls, therefore reducing the risk of failure of the structure under extreme wave conditions. Figures 11 shows the maximum pressures on the back OWC wall, pressures are reduced substantially in the U-OWC, and these pressures are relatively insensitive to U-wall height.

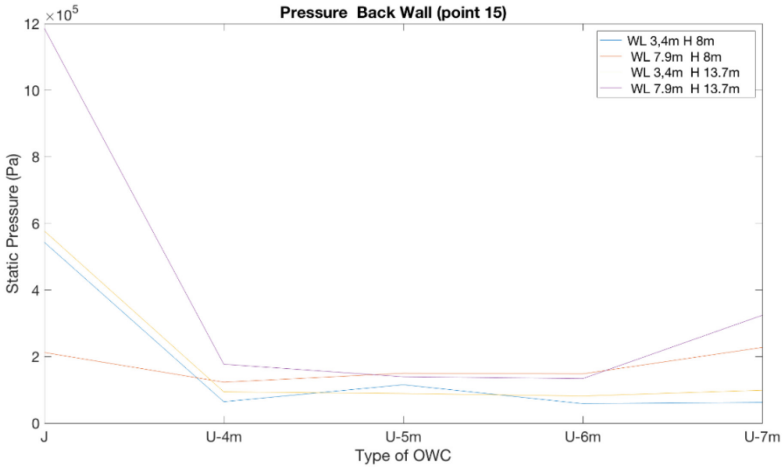

Fig. 11. Comparison of the maximum internal pressures on the internal back wall for the different geometries and wave conditions.

5.3 Power production by the OWC

Figure 12 shows the wave height inside the OWC for the storm conditions considered. It is seen that there is a reduction of the average wave height in the column from the J-OWC to the U-OWC and also as the U-wall height increases.

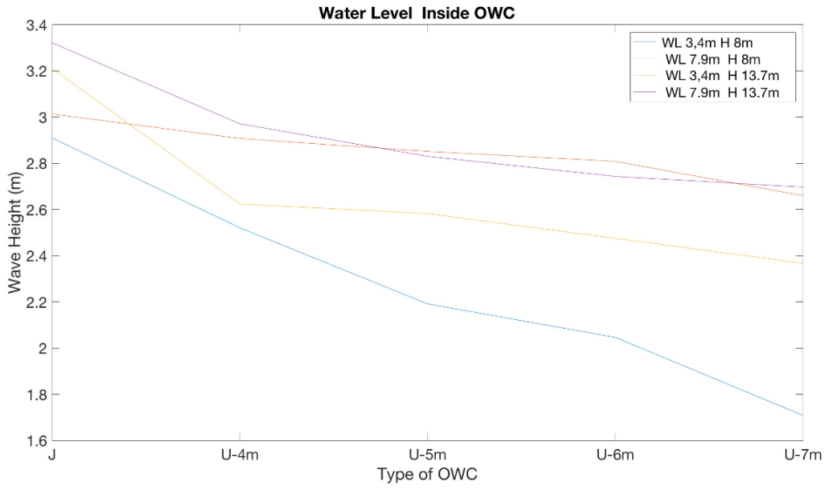

Fig. 12. Wave height inside the OWC for storm conditions.

6 References

ANSYS, 2009. Theory Reference. s.l.:Release 5.6 .

Arena, F., Romolo, A., Malara, G. & Ascanelli, A., 2013. On Design and Building of a U-OWC Wave Energy Converter in the Maditerranean Sea: A Case Study. ASME 2013 32nd International Conference on Ocean, Offshore and Arctic Engineering (pp. V008T09A102-V008T09A102), American Society of Mechanical Engineers..

Berenguer, 2009. Memoria: Proyecto básico de reparación de la central undimotriz del puerto de mutriku. Bilbao: Gobierno Vasco .

Boake, C. B., Whittaker, T. J. T. & Folley, M., 2002. Overview and Initial Operational Experience of the LIMPET Wave Energy Plant. Japan, s.n.

Czech, B. & Bauer, P., 2012. Wave energy converter concepts: Design challenges and classification. IEEE Industrial Electronics Magazine, 6(2), pp. 4-16.

Elhanafi, A. & Joo Kim, C., 2018. Experimental and numerical investigation on wave height and power take-off damping effects on the hydrodynamic performance of an offshore-stationary OWC wave energy converter. Renewable energy, Issue 125, pp. 518-528.

Falcao, A. F. d. O., 2010. Wave energy utilization: A review of the technologies. Renewable and sustainable energy reviews, 3(899-918), p. 14.

Kamath, A., Bihs, H. & Arntsen, O. A., 2015. Numerical investigations of the hydrodynamics of an oscillating water column device. Ocean Engineering, Issue 102, pp. 40-50.

Müller, G., & Whittaker, T. J. (1995). Visualisation of flow conditions inside a shoreline wave power-station. Ocean engineering, 22(6), 629-641.

Mustapa, M. A. et al., 2017. Wave energy device and breakwater integration: A review. Renewable and Sustainable Energy Reviews, Issue 77, pp. 43-58.

Torkar, K. & Jeszenszky, H., 2006. Midas User Manual. s.l.:IWF.

Torre-Encino, A., Marqués, J. & López de Aguileta, L., 2010. Mutriku Lessons learnt. Bilbao, ICOE.

Webb, I., Seaman, C. & Jackson, G., 2005. Oscillating Water Column Wave Energy Converter Evaluation Report. Marine Energy Challenge - The Carbon Trust.